Analysis of Wireless Optical Communications Feasibility in Presence of Clouds Using Markov Chains

Z. Hajjarian, *Member, IEEE*, M. Kavehrad, *Life Fellow, IEEE*, and J. Fadlullah, *Member, IEEE*

***Abstract*—Free Space Optical (FSO) communications is a practical solution for creating a three dimensional global broadband communications grid, offering bandwidths far beyond possible in Radio Frequency (RF) range. However, attributes of atmospheric turbulence (scintillation) and obscurants such as clouds impose perennial limitations on availability and reliability of optical links. To design and evaluate optimum transmission techniques that operate under realistic atmospheric conditions, a good understanding of the channel behavior is necessary.**

In most prior works, Monte-Carlo Ray Tracing (MCRT) algorithm has been used to analyze the channel behavior. This task is quite numerically intensive. The focus of this paper is on investigating the possibility of simplifying this task by a direct extraction of state transition matrices associated with standard Markov modeling from the MCRT computer simulations programs. We show that by tracing a photon's trajectory in space via a Markov chain model, the angular distribution can be calculated by simple matrix multiplications. We also demonstrate that the new approach produces results that are close to those obtained by MCRT and other known methods. Furthermore, considering the fact that angular, spatial, and temporal distributions of energy are inter-related, mixing time of Monte-Carlo Markov Chain (MCMC) for different types of aerosols is calculated based on eigen-analysis of the state transition matrix and possibility of communications in scattering media is investigated.

***Index Terms*—Angular Dispersion, Channel Modeling, Markov Chain, Monte-Carlo Ray Tracing, Scattering, Second Largest Eigen Modulus (SLEM).**

I. Introduction

FREE Space Optical (FSO) communications is the only practical solution for creating a broadband three-dimensional global communications grid among ground and airborne nodes, due to its ease of deployment, enormous available bandwidth, possibility of reuse, and inherent security at physical layer, as laser beams are normally spatially confined and cannot be tapped [1], [2]. In ideal free-space, the total loss due to absorption and scattering is virtually zero. This is because of the spatial confinement of laser beams. However, atmospheric obscurants such as; fog, haze, smoke, dust and clouds turn the propagation environment into a multiple scattering medium and hence introduce laser pulse broadening in space and time. Moreover, even in clear weather, turbulence due to refractive index fluctuations in layers of atmosphere causes scintillation, introducing both phase and intensity distortions across the transmitted light beam [3], [4]. In presence of multi-scattering, both availability and capacity of optical link degrade, significantly. The focus of this paper is on deleterious effects of scatterings and aerosols. Turbulence-induced scintillation is not further discussed in this paper.

In some applications, transmit power is limited, in order to observe eye and skin safety regulations and on the other hand, sensitivity of optical receivers is affected by the shot noise caused by background light [5]. Hence, link budget management becomes very critical and challenging. Furthermore, multi-path delay spreading limits the achievable bit rates [6]. In digital FSO communications, one is usually interested in the peak power of received waveform in order to distinguish the signal from steady background radiation [7], [8]. In a receiver unequipped with appropriate countermeasure techniques, overlapping of pulse tails on adjacent symbol intervals introduces intersymbol-interference (ISI), and thus limits the achievable bit rate. As a result, receiver should have a small Field-of-View (FOV) and has to resort to Line-of-Sight (LOS) photons, known as ballistic, and/or near LOS (snake) photons which are highly forward scattered. However, if due to thickness and/or particle density of obscurants, light pulse enters the diffusion regime, spatial distribution approaches a normal distribution and angular distribution becomes isotropic [9]. In this case, a receiver of small FOV may fail to maintain the desired link margin.

To answer the fundamental question of optical communications feasibility in presence of clouds, one has to accurately model atmospheric optical channel and estimate parameters such as angular, spatial, and temporal dispersions.

As a collimated laser beam propagates through clouds, it spreads and after traveling some distance, it reaches a steady state of being defocused and diffused. The rate of convergence to this steady state determines feasibility of communications through various clouds of different optical thickness values. Optical thickness τ is the average number of scatterings over a given length of cloud whose value is a number with no physical unit. It is defined by multiplying the scattering coefficient, β_{sca} (km^{-1}), of cloud by the physical cloud length, L, in km. We will elaborate on this issue more, in section-II.

So far, Monte-Carlo Ray Tracing (MCRT) has been used to calculate the channel parameters [7], [10], [11], [12], [13]. This method requires a high computational capacity and a long execution time. In [9], authors find spatial and angular

Manuscript received 15 January 2009; revised June 18, 2009.

M. Kavehrad is with the Department of Electrical Engineering, Pennsylvania State University, University Park, PA, 16802 USA (e-mail: mkavehrad@psu.edu).

Z. Hajjarian and J. Fadlullah are with the Department of Electrical Engineering, Pennsylvania State University, University Park, PA, 16802.

Digital Object Identifier 10.1109/JSAC.2009.091202.

distribution by a statistical approach. However, their results are limited to the first two moments of multiple scattering. Finding angular distribution is of great importance in computer graphics, as well. In [14], a single-scatter impulse response is defined for and then the result is generalized to multiple scattering via convolution. Since this impulse response is three dimensional, convolution process is quite cumbersome. In this paper, angular distribution evolution of a laser beam in a multiple scattering medium is characterized by extracting the corresponding simplified Markov chain information from the MCRT algorithm. By calculating the state transition matrix, one can find the probability distribution function of scattering angle after any number of scatterings. We show that the Markov chain model produces values that are close to MCRT results and other proposed analytical methods, yet need much less time to produce the results. Since angular, spatial and temporal distributions of received power are inter-related, useful information can be extracted from angular distribution about the behavior of the entire system. The remainder of this paper is organized as follows. In section-II, Mie scattering theory is reviewed. Section-III applies Markov chain model to laser beam propagation and derives and demonstrates the state transition matrix for cumulus clouds. Results are presented in section-IV and section-V contains eigen-analyses of the state transition matrix. Finally section-VI presents a summary and concludes the paper.

II. Mie Theory Of Scattering And Phase Function

When propagating through clouds or fog, a laser beam interacts with medium particles, which are mostly water droplets of sizes comparable to the optical wavelength values. Hence, we need Mie theory to explain these interactions. This theory is the application of Maxwell's equation to the problem of a homogeneous sphere radiated by a plane wave from a single direction [15]. Knowing particle size distribution of the medium, one can determine absorption, extinction, and scattering coefficients as well as phase function, using this theory. Assuming that particles are homogeneously distributed in space, distance between two successive scatters turns out to be an exponential random variable with a mean value of $D_{ave} = \frac{1}{\beta_{sca}}$, where β_{sca} is the scattering coefficient. Furthermore, absorption, extinction, and scattering coefficients are related as: $\beta_{sca} + \beta_{abs} = \beta_{ext}$, where β_{abs} and β_{ext} are absorption and extinction coefficients, respectively. Additionally, the ratio of the scattered energy to the total energy is determined by single scatter albedo, $\varpi = \frac{\beta_{sca}}{\beta_{ext}}$.

According to Mie theory, one can define the scatter direction via a three-dimensional probability distribution function (PDF) known as the *Phase Function*. In other words, *Phase Function* is the PDF of the solid angle $\Omega = (\theta, \phi)$ [15], [16], [17]. For example, in [16] we find that:

$$\int_{Over\ 4\pi} P(\theta)d\Omega = \int_0^{\pi}\int_0^{2\pi} P(\theta)\sin(\theta)d\theta d\varphi = 4\pi \quad (1)$$

where $P(\theta)$ in equation (1) is referred to as the (unnormalized) scattering phase function in the literature.

Fig. 1 demonstrates the scattering phase function for different kinds of clouds. These phase functions are obtained by substituting the modified gamma distribution for radius density of cloud particles in equations extracted from Mie theory for poly-dispersed phase function [15], [18]. It is clear from this figure that all these phase functions are highly-peaked in the forward direction. Actually, since the azimuth scattering angle, φ, is uniformly distributed in $[0, 2\pi]$, the *Phase Function* can be plotted only against the polar scattering angle, θ.

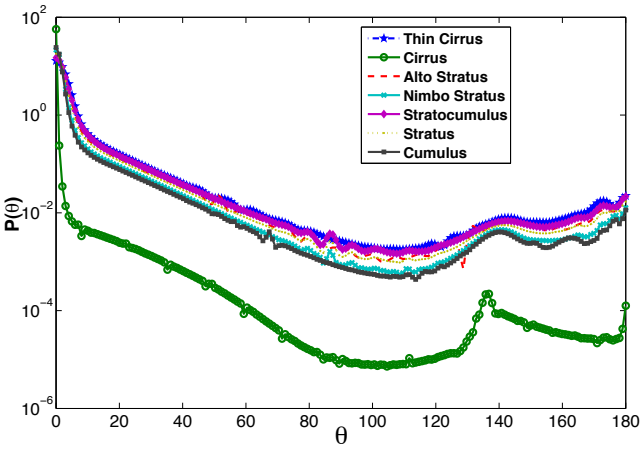

Fig. 1. Phase functions for different types of clouds.

Scattering phase function can also be interpreted as the PDF of $\cos(\theta)$ [10], [17].

In order to find suitable probabilities to inject into a Monte Carlo model, one needs the probability density function of θ, not the plotted scattering phase functions. The normalized phase function, as generally used in the literature, is normalized so that its integration over all possible scatter angles (4π steradians) is unity, thus qualifying it to be a PDF. With no φ dependence of $P(\theta)$, the integration over φ simply contributes a factor of 2π. This leads to normalization definition for $P(\theta)$ of:

$$2\pi \cdot \int_0^{\pi} \frac{P(\theta)}{4\pi} \cdot \sin(\theta)d\theta = \int_0^{\pi} P(\theta) \cdot \frac{\sin(\theta)}{2} \cdot d\theta = 1.$$

Thus, PDF of θ can be extracted from the normalized phase function and be expressed as:

$$f(\theta) = P(\theta) \cdot \frac{\sin(\theta)}{2}. \quad (2)$$

Unfortunately, expressing the phase function versus θ has caused a great deal of confusion in the published literature [19], [20]. More specifically, several authors have mistaken the phase function for the PDF of θ and obtained an extremely forward directed angular distribution of scattered beams, which is incorrect.

For example, in the case of isotropic scattering, by mistaking the phase function for PDF of θ, one may think that θ is uniformly distributed in $[0, \pi]$. However, it is the phase function (PDF of solid angle Ω) that is uniform and θ is distributed as $f(\theta) = P(\theta)\sin(\theta)/2$ [17], [19], [20].

In order to obtain a better understanding of multiple scattering mechanisms, one may wish to use an approximate phase function that can be easily parameterized and is more convenient to use than Mie series [7]. The most popular

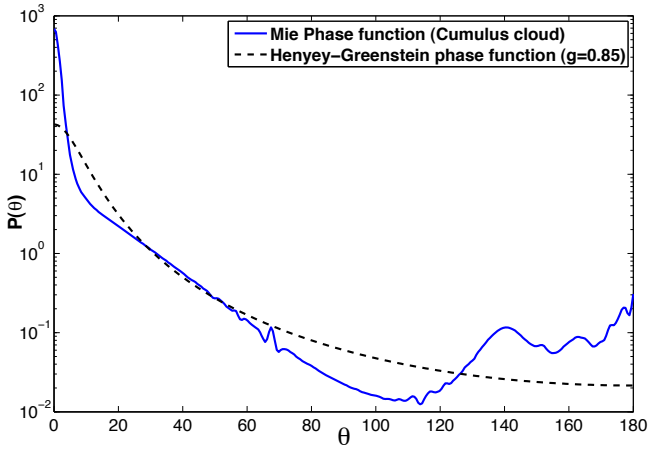

Fig. 2. Henyey-Greenstein phase function for a cloud of $g = 0.85$.

approximate phase function is the Henyey-Greenstein (HG) scattering function [21] and is given by:

$$P(\theta) = \frac{(1-g^2)}{2\pi(1-2g\cos\theta+g^2)^{3/2}}.$$

This approximate phase function is completely characterized by the parameter g, which is the average value of $\cos(\theta)$, and is also called the asymmetric parameter. As we see later in this paper, the asymmetric parameter is of great importance since it determines the convergence rate of the Markov chain associated with density evolution of polar angle, θ. In Table-I is listed the parameter g for different clouds. The data has been acquired using phase functions of Fig. 1 and finding the corresponding average values for $\cos(\theta)$. For most clouds, $\overline{\cos(\theta)} \approx 0.85$, and for more forward-scattering clouds, $\overline{\cos(\theta)} \approx 0.995$ as stated in [9]. Fig. 2 shows the HG phase function for a cloud of $g = 0.85$. Clearly, HG phase function does not contain all the details of scattering function and is much smoother than the full Mie series phase function. However, results obtained from MCRT algorithm using these two scattering functions are quite similar [7].

Mie theory, although very useful in describing single scattering phenomena, does not provide sufficient insight into the multiple scattering problems by itself. Instead, one should exploit this theory along with a powerful tool to explain laser beam propagation in a multi-scattering medium. MCRT is one such method that is based on brute-force tracking of all photons' trajectories in a three dimensional space. As a result, it is quite numerically intensive.

In the next section, we describe our new approach of channel modeling, which is based on direct extraction of state transition matrices associated with standard Markov modeling from the MCRT computer simulations programs.

III. Model

Having reviewed Mie scattering theory, now we can model photon trajectory as a random walk using Markov chain, and investigate evolution of angular beam spreading. If we consider laser beam to be composed of a large body of coherent photons traveling in the same direction, by tracking these photons, one can account for laser beam propagation in a multiple scattering medium. MCRT algorithm implements this brute-force tracking. Fig. 3 shows the geometry of multiple scattering.

TABLE I
Asymmetric Parameter for Different Clouds at a Wavelength of $\lambda = 1.55\mu m$

Cloud	Asymmetric Parameter
Thin Cirrus	0.82
Cirrus	0.87
Alto Stratus	0.83
Nimbo Stratus	0.85
Stratocumulus	0.82
Stratus	0.83
Cumulus	0.85
HG (g = 0.85)	0.85
HG (g =0.95)	0.95

Note that, in Fig. 3 the indexed and primed 3-tuples, $(d_k^{'}, \theta_k^{'}, \varphi_k^{'})$, represent random variables associated with the k^{th} scattering event in local spherical coordinates, and should not be confused with variables associated with the k^{th} state of the Markov process, described later. In other words, considering the finite-state machine concept, the indexed and primed 3-tuples, $(d_k^{'}, \theta_k^{'}, \varphi_k^{'})$ are the inputs to the system at the k^{th} step. Later in this paper, we will use indices to refer to the state variables; hence, we will drop the prime and index of the input variables for simplicity, as these variables are independently generated at each step, according to some fixed probability density functions.

Note that, the notion of photon simply refers to a packet of energy (or a very small portion of the beam) in the MCRT context and we are not dealing with Quantum Mechanical aspects of photons.

To describe the MCRT algorithm and our Markov chain model, first we clarify our notations and terminologies. In MCRT, the k^{th} state of a photon, i.e. a photon's position and directions in global coordinate system right before the $(k+1)^{th}$ scattering event, is specified by $[x_k, y_k, z_k, \theta_k, \varphi_k]$ where (θ_k, φ_k) represent the traveling direction in global spherical coordinates and (x_k, y_k, z_k) stands for position in global Cartesian coordinates. Note that, direction can also be expressed by directional cosines (μ_x, μ_y, μ_z) in the global Cartesian coordinate system [17]; however, we choose the former notation because it requires only two variables and fits better in our simplified Markov chain model. After $(k+1)^{th}$ collision, a photon is deflected with angles (θ, φ) in local coordinates, (i.e. pre-collision traveling direction is the local z axis) and travels a distance d, until it goes through the next scattering event. Hence, the $(k+1)^{th}$ state of this photon can be determined using its previous state and the new input to the system, which is the 3-tuples (d, θ, φ). We have dropped the index and prime of this 3-tuple for simplicity, as we need the indices to specify the states. Note that, some authors [9] used a different notation in that they indexed the input 3-tuples (d, θ, φ) measured with respect to local coordinate system, however, in order to define the Markov chain model, we choose to index the states, which are measured with respect to global coordinate system.

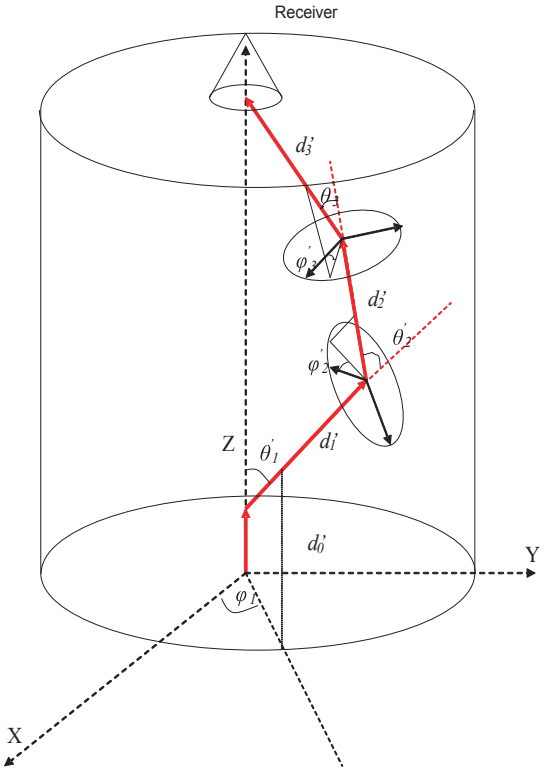

Fig. 3. Geometry of multiple scattering.

MCRT calculates channel parameters such as angular, spatial, and temporal dispersions using statistics of photons reaching the receiver plane in a post-processing stage.

In the Markov chain of MCRT, variables associated with the position of a photon in a three-dimensional space are neither finite, nor countable. However, if we limit our attention to photons' direction in spherical coordinates, and quantize θ, a finite state Markov chain is obtained. Note that, due to symmetry, azimuth traveling direction, φ, is always uniformly distributed in $[0,\ 2\pi]$. Furthermore, if it is assumed that the laser beam is traveling in a homogeneous medium, the phase function will not change from one state to the next. Thus, a Markov chain with a time-invariant state transition matrix can represent the angular distribution evolution of laser beam, while it is traveling through a multiple scattering medium.

We claim that the angular dispersion, defined as the average cosine of the incidence angle on the receiver plane, can be calculated by modeling the photon trajectory in a 3-D space by a random walk. Moreover, this method provides us with the complete angular distribution, rather than just the moments. Also, it is superior to MCRT since due to its analytical nature, it is more tractable. Furthermore, in MCRT, a large number of photons are sent into the scattering medium with the hope of finding the distribution of photons on the receiver plane. Hence, to account for all possible paths and angles, a large amount of processing is required that may not be desirable. While computational complexity of MCRT is very high and computer simulation programs need a large execution time, this analytical method can provide us with results for angular distribution through simple matrix multiplications.

Suppose a photon is traveling in the θ_{k-1} direction with respect to z axis before k^{th} scattering. If this photon collides with a cloud particle, its propagation direction changes in space. Fig. 4 illustrates the geometry of the problem. The change in direction is described by the phase function. However, phase function provides the PDF of the cosine of deflection angle with respect to initial traveling direction, while we are interested in a traveling direction with respect to the global z axis. In other words, a phase function provides us with a distribution for $\cos(\theta)$, while we want the distribution of θ_k, as in Fig. 4. The term $\cos(\theta_k)$ is related to $\cos(\theta_{k-1})$ via:

$$\cos\theta_k = \cos\theta_{k-1}\cos\theta - \cos\varphi\sin\theta_{k-1}\sin\theta, \tag{3}$$

where θ and φ are polar and azimuth scattering angles, respectively. While φ is uniformly distributed over $[0,\ 2\pi]$, the distribution of θ is given by $P(\theta)\sin(\theta)/2$. To determine the probability distribution function of θ_k, first we determine its cumulative distribution function.

$$\begin{aligned}&\Pr(\theta_k < \xi) = \Pr(\cos\theta_k > \cos\xi) = \\ &\Pr(\cos\theta_{k-1}\cos\theta - \cos\varphi\sin\theta_{k-1}\sin\theta > \cos\xi)\end{aligned} \tag{4}$$

Hence, we can write

$$\begin{aligned}&\Pr\left(\cos\varphi < \frac{\cos\xi - \cos\theta_{k-1}\cos\theta}{-\sin\theta\sin\theta_{k-1}}\right) = \\ &\Pr\left(\varphi > \cos^{-1}\left(\frac{\cos\xi - \cos\theta_{k-1}\cos\theta}{-\sin\theta\sin\theta_{k-1}}\right)\right)\end{aligned} \tag{5}$$

Finally, the cumulative distribution can be expressed as:

$$\begin{aligned}&\Pr(\theta_k < \xi) = \\ &\int_0^{\pi} f(\theta)\int_{\cos^{-1}\left(\frac{\cos\xi - \cos\theta_{k-1}\cos\theta}{-\sin\theta\sin\theta_{k-1}}\right)}^{2\pi} f(\varphi)d\varphi d\theta = \\ &\int_0^{\pi} P(\theta)\sin\theta\left(1 - (2\pi)^{-1}\cos^{-1}\left(\frac{\cos\xi - \cos\theta_{k-1}\cos\theta}{-\sin\theta\sin\theta_{k-1}}\right)\right)d\theta\end{aligned} \tag{6}$$

If we differentiate the last equation, we obtain the PDF of θ_k.

It is also possible to directly generate PDF of θ_k, by rewriting equation (3) as:

$$\begin{aligned}&\cos(\theta_k) = \\ &\cos(\varphi/2)^2\cos(\theta_{k-1}+\theta) + \sin(\varphi/2)^2\cos(\theta_{k-1}-\theta)\end{aligned}. \tag{7}$$

Then, the PDF of θ_k can be found by adding up the probabilities associated with all values of θ and φ that give rise to a certain θ_k, given θ_{k-1}.

Now, we can form a matrix with its rows corresponding to incident angles and its columns corresponding to scattering angles. This matrix can be used as the state transition matrix of the Markov process. Equation (8) illustrates this matrix.

$$P = \begin{bmatrix} P(\theta_k = 0|\theta_{k-1} = 0) & \dots & P(\theta_k = \pi|\theta_{k-1} = 0) \\ \vdots & & \vdots \\ \vdots & \dots & \vdots \\ \vdots & & \vdots \\ P(\theta_k = 0|\theta_{k-1} = \pi) & \dots & P(\theta_k = \pi|\theta_{k-1} = \pi) \end{bmatrix} \tag{8}$$

If one wishes to know distribution of a photon's direction after k^{th} scattering event, knowing that it was initially traveling in the z direction, one has to calculate

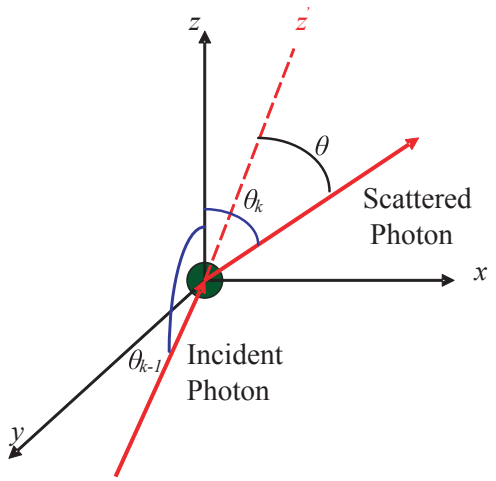

Fig. 4. Relationship between θ_{k-1}, θ and θ_k.

$$P_k(\theta) = (P^K)^T \begin{bmatrix} 1 \\ 0 \\ . \\ . \\ . \\ 0 \end{bmatrix} \tag{9}$$

First row of the state transition matrix is $P(\theta)\sin(\theta)/2$. Hence, we can find the phase function resulting from k scattering events from the first row of k^{th} power of state transition matrix, simply by taking out the $\sin(\theta)/2$ factor.

Fig. 5 shows the state transition matrix for cumulus cloud at a wavelength of *1.55 μ m*. We have calculated the state transition matrix with a resolution of $\pi/300$. In other words, P is a 300 $\times$ 300 matrix. We observed that by increasing the resolution to $\pi/1000$, our simulation results do not change.

The forward scattering property of cumulus cloud is clear from this picture. That is, the state transition matrix is very close to an identity matrix. Fig. 6 shows P^{15} which clarifies transition probabilities at an optical thickness value of 15. Here, the value 15 is chosen since for this value, there are less line-of-sight (LOS) photons, and most of the photons that may reach the receiver have gone through multiple-scatterings. From Fig. 6, one can see that after 15 scattering events, the phase surface is very close to the shape of $\sin(\theta)/2$. This corresponds to an isotropic scattering. Fig. 7 shows a side view of the phase surface. One can observe that different rows of the matrix are very close but, not as yet identical.

Fig. 8 shows P^{50}, that is, the phase surface after 50 scattering events. This figure clearly illustrates isotropic radiation after 50 scattering events. Fig. 9 shows a side view of phase surface. It can be inferred that after 50 scattering events, irrespective of the initial incident angle value, the scattering angle is distributed as $\sin(\theta)/2$. This is consistent with Bucher's [6] observation of uniform brightness of the cloud bottom.

IV. Results

As mentioned earlier, application of Markov chain in MCRT cloud modeling is a shortcut for calculating the angular distribution of energy in space for any arbitrary optical thickness.

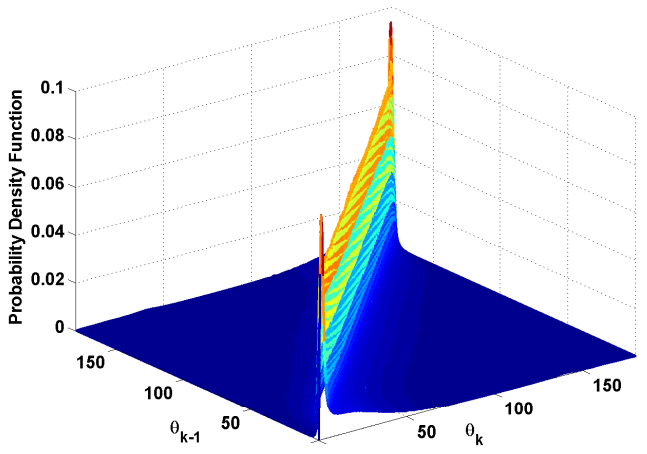

Fig. 5. State transition matrix of cumulus clouds at a wavelength $\lambda = 1.55\mu m$.

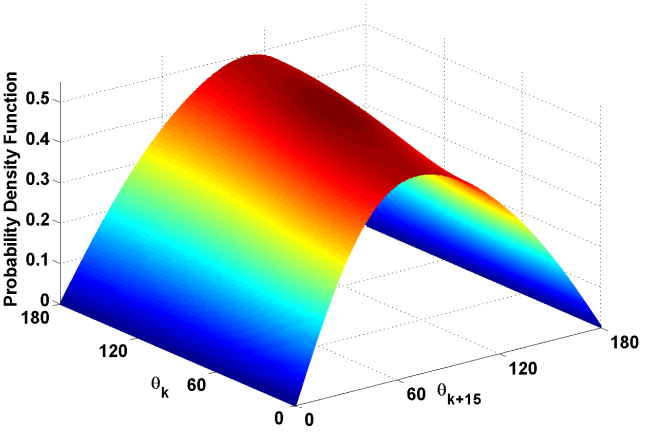

Fig. 6. State transition matrix of cumulus cloud, raised to 15th power, at a wavelength= $1.55\mu m$.

In this section, we compare the results of our Markov chain model with those of MCRT and another analytical method, which we call the moment technique [9].

To make a fair comparison, we note that while both MCRT and Markov chain model produce a complete distribution, the moment technique only comes up with the first two moments. Furthermore, MCRT can provide us with the distribution of photons on the receiver plane.

However, both Markov chain model and moment technique generate angular distribution in a three-dimensional space, i.e. on a sphere. Hence, to compare the Markov chain model with MCRT, we should only consider the forward part of the distribution, i.e., $0 < \theta < \frac{\pi}{2}$. Moreover, we should take into account the projected area correction factor of $\cos(\theta)$ for mapping from a 3-D distribution on a sphere onto a 2-D distribution on the receiver plane [7].

Given a photon at the cloud exit plane has been subject to scattering k times over a cloud length L, its angular distribution would be $P_k(\theta)$ as in equation (9).

To calculate the unconditional angular distribution, we note that the probability that a photon undergoes exactly k scatterings over L is Poisson distributed with a mean τ, where τ is the optical thickness, as defined earlier. That is:

$$P(K(\tau) = k) = \frac{\tau^k}{k!} e^{-\tau} \tag{10}$$

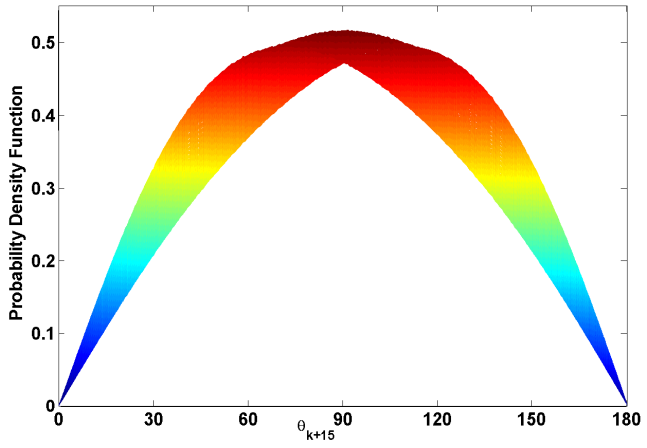

Fig. 7. Side view of the state transition matrix, raised to 15th power.

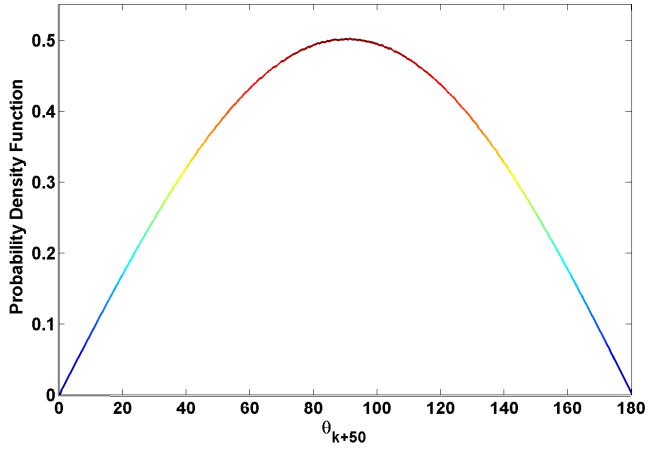

Fig. 9. Side view of the state transition matrix, raised to 50th power.

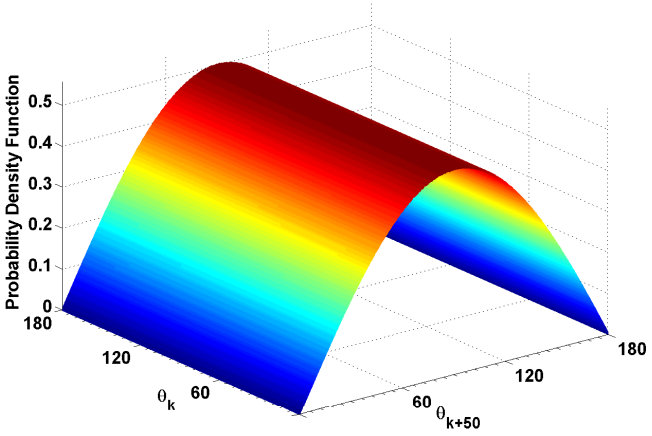

Fig. 8. State transition matrix of cumulus cloud, raised to 50th power, at a wavelength= $1.55\mu m$.

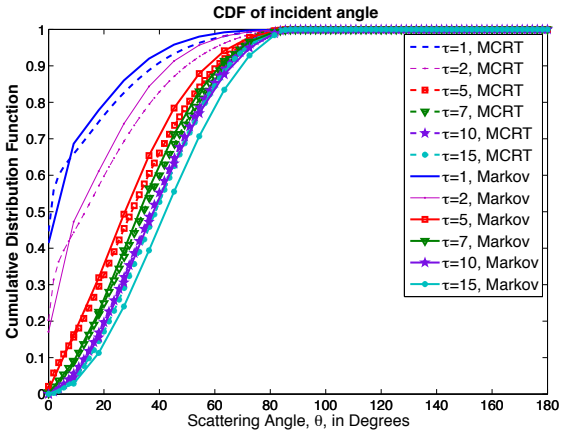

Fig. 10. **Comparison of *CDF* curves for angular distribution.**

Hence, the angular distribution for this optical thickness value is:

$$P(\theta) = \sum_{k=0}^{\infty} \frac{\tau^k}{k!} e^{-\tau} . P_k(\theta) \tag{11}$$

Using equation (11), angular distribution is calculated for optical thickness values of 1 to 15. Fig. 10 shows the cumulative distribution function (CDF) of incident angle obtained from Markov chain model and MCRT, where we have applied the above-mentioned measures in order to make the comparison fair. From Fig. 10, one can see that CDF curves obtained from Markov chain model and MCRT are quite close in numerical values. Furthermore, as optical thickness value increases, angular dispersion increases.

One important measure of angular dispersion is the average cosine of incident angle, $\overline{\cos(\theta)}$. Variance of cosine of incident angle is also considered as a measure of angular dispersion in the literature. The moment technique provides us with the first two moments of $\cos(\theta)$ in a three-dimensional space. However, MCRT provides the complete distribution on the receiver plane. Then, one can find the first two moments of $\cos(\theta)$ using this distribution.

The Markov chain model, in its original shape, produces the same mean and variance as those of the moment technique. However, as mentioned earlier, it can be truncated and modified to provide the distribution on the receiver plane. Figs. 11 and 12 show the mean and the variance of $\cos(\theta)$ for MCRT, truncated Markov, original Markov, and moment technique (labeled 'Moments') for different optical thickness values.

It is clear from these figures that the variance of the cosine of incident angle increases with optical thickness, whereas the mean decreases. This implies that for small optical thickness values, a receiver of small FOV suffices to collect the required power; however, for large optical thickness values, the energy is almost uniformly distributed in a 3-D space. Saturation of variance curves in Figs. 11 and 12 suggests that density evolution of angular distribution merges to the steady-state and the Markov chain converges to the equilibrium distribution. It is also evident from these figures that our Markov chain model is consistent with both MCRT and moment technique.

Finally, the time required for each method to generate the results in different optical thickness values is tabulated in Table-II. Computer programs were executed on a 3.40 GHz Pentium-4 CPU, with 2.00 GB of RAM. It is clear from this table that the computation time for MCRT increases with the optical thickness value. However, neither the Markov chain model, nor the moment techniques show much variability in

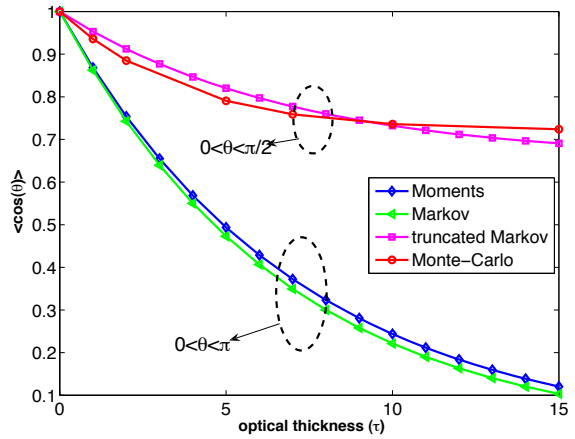

Fig. 11. **Comparison of $\overline{\cos(\theta)}$ for different methods.**

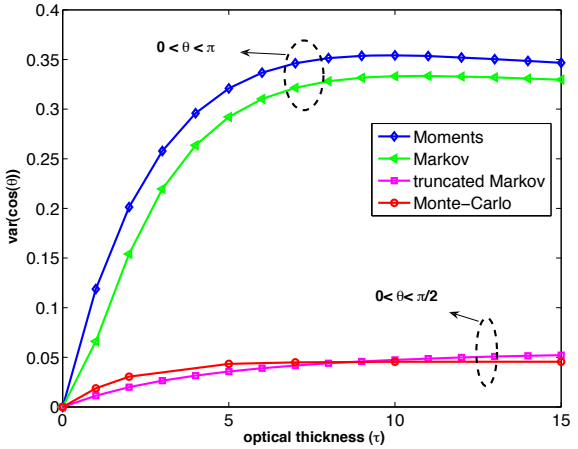

Fig. 12. **Comparison of $var(\cos(\theta))$ for different methods.**

the computation times, for different optical thickness values. We also note that the execution time required for the Markov chain model is significantly less than MCRT but much more than moment technique. However, moment technique gives only the first two moments, and not the complete distribution. Thus, the Markov chain model is able to demonstrate a more complete picture.

Note that, running time of MCRT increases exponentially with the optical thickness of the scattering media. For large optical thickness values, the running time will no longer be reasonable. Furthermore, running time of MCRT also depends on the number of photons, the positions and directions of which at each scattering location have to be recorded. Again, by increasing the number of these photons, running time increases. The program is terminated when the number of received photons is large enough so that the statistical variations at receiving plane become negligible.

The main point of this paper is not to substitute for or compete with the comprehensive Monte-Carlo method by the less time-consuming Markov chain model. We are seeking new insight into the problem of laser beam propagation in scattering media. The trend of how fast a collimated laser beam diverges into a completely diffuse light source is more

TABLE II
RUNNING TIME OF THREE METHODS FOR DIFFERENT OPTICAL THICKNESS VALUES

Optical Thickness	MCRT	Markov	Moments
1	656 s	33 s	0.06 s
5	767 s	33 s	0.06 s
10	948 s	33 s	0.06 s
15	1212 s	33 s	0.06 s

easily observed using the proposed Markov chain model. Also, the concept of eigenvalues of this Markov chain process is better understood this way. These are critical facts from a communications point of view; pulse broadening in space and time is and will continue to be the major limitation for high-speed communications in scattering media.

V. EIGEN ANALYSES

State transition matrix,P has no zero entries, and hence is regular. In other words, it is possible to go to all the states from any arbitrary state. It is a well known fact that for a regular Markov chain, as n approaches infinity, $P^n = \Pi$, where Π is a matrix of the form [ν, ν, ..., ν], with ν being a constant vector.

From the previous section, we see that this is true about state transition matrix of our Markov chain P, and as n increases, all the rows of the state transition become identical and proportional to $\sin(\theta)/2$. Now, the question is whether it is possible to predict ν, and thus Π, without using the limits and the answer is affirmative. In fact, Π satisfies the equation:

$$\Pi P = \Pi, \tag{12}$$

Notice that, from Perron-Frobenius theorem [22], ν is the first left eigenvector of P, corresponding to the unique largest eigenvalue, $\lambda_0 = 1$. By examining the first left eigenvector of matrix P, we realize that it is proportional to $\sin(\theta)/2$. Hence, we could have predicted the diffuse behavior of light at the bottom of cloud, just by looking at the left eigen vector of state transition matrix, to start with.

Convergence of P^k elements means that it becomes more and more difficult to guess k, from p_{ij}^k (the element in the i^{th} row and the j^{th} column of P^k). That is, the chain forgets the length of its history [22]. The fact that limit of P^k has identical rows suggests that the Markov chain forgets the initial direction.

When a Markov chain converges to this steady-state, traveling direction of photons becomes rather isotropic, as opposed to forward-scatter in initial steps. This suggests that the laser beam is spatially diffused and irrespective of initial traveling direction, photons escape almost uniformly from all boundaries of the cloud. In this case, spatial confinement of transmitted energy is no longer preserved and loss (mostly attributed to scattering) is rather large.

In some applications, due to eye safety regulations, there is restriction on increasing the transmit power level beyond a certain maximum. Under such circumstances, receiver may not see much forward scatter (snake) photons and must resort

to only the LOS (ballistic) photons, that is, the non-diffused part of the intensity, which is attenuated according to Beer-Lambert law as:

$$I_{coh} = I_0 e^{-\tau}, \tag{13}$$

Needless to say, by using ultra-short laser pulses and cascade amplifiers, this component can be amplified, significantly. In equation (13), τ is the optical thickness of cloud, as defined earlier.

The number of steps required for the Markov chain to converge to the equilibrium state is of great importance since it determines the depth up to which the laser beam can penetrate before becoming spatially diffused.

From equation (3), one can see that:

$$\overline{\cos(\theta_k)} = \overline{\cos(\theta_{k-1})} \times \overline{\cos(\theta)} = g\overline{\cos(\theta_{k-1})} = g^k \tag{14}$$

In other words, the asymmetric parameter, g determines the convergence rate of Markov chain. On the other hand, from the Markov chain theory [23], we know that the Second Largest Eigenvalue Modulus (SLEM) determines the "Mixing Rate" of a Markov chain. In other words, the smaller the SLEM is, the faster the spatial memory-loss happens. Hence, "Mixing-Time" of a Markov chain is given by:

$$T = \frac{1}{\log\left(\frac{1}{\lambda_*}\right)} \tag{15}$$

where T is the number of steps over which deviation from equilibrium state decreases by a factor e, and λ_* is the SLEM. By examining the eigenvalues of P (state transition matrix of cumulus cloud) we realize that the second largest eigenvalue is indeed the asymmetric parameter g.

Table - III lists the SLEM for Markov chains associated with HG phase functions of different asymmetric parameters as well as full Mie series phase function for different types of clouds. This table also contains the mixing time and the average distance between two successive scattering events for each cloud. Average distance, D_{ave}, between two successive scattering events is used to convert optical thickness of a specific scattering medium to its physical thickness and vice versa. It also corresponds to the inverse of scattering coefficient, expressed in km^{-1}, which can be obtained by substituting the cloud particle size distribution in equations extracted from Mie theory for poly-dispersed extinction coefficient [18], [24]. From Table - III we see that the second largest eigenvalue is equal to g for all of these phase functions. That is why asymmetric parameter is important in calculating the moments of multiple scattering and channel parameters [7], [9]. Since angular, spatial and temporal distributions of energy are inter-related, isotropic angular distribution suggests that spatial distribution in transverse coordinates (x and y directions) is Gaussian. Furthermore, spatial memory-loss of Markov chain associated with angular distribution after several scattering events implies that the entire Monte-Carlo Markov chain (MCMC) has converged to the equilibrium state. This suggests that the pulse is so broadened in space and time that use of equalization on the pulse might be difficult, unless there is no constraint on the optical transmitted peak power level.

TABLE III
ASYMMETRIC PARAMETER & SLEM FOR DIFFERENT CLOUDS AT A WAVELENGTH OF $\lambda = 1.55\mu m$

Cloud	SLEM	g	Mixing Time	D_{ave}
Thin Cirrus	0.82	0.82	5	11.3 km
Cirrus	0.87	0.87	7	984 m
Alto Stratus	0.83	0.83	5.4	10.5 m
Nimbo Stratus	0.85	0.85	6.2	12.3 m
Stratocumulus	0.82	0.82	5	26.5 m
Stratus	0.83	0.83	5.4	17.5 m
Cumulus	0.85	0.85	6.2	7.5 m
HG(g=0.85)	0.85	0.85	6.2	N/A
HG (g=0.95)	0.95	0.95	19.5	N/A
Low Altitude Haze	0.73	0.73	3.2	817.8 m
Medium Altitude Haze	0.78	0.78	4	238.8 m

Examining parameters of Table - III, we realize that mixing time is rather short for clouds and haze and a large link margin is necessary, in order to have reliable communications through clouds of optical thickness values much larger than 10 to 15. However, this rather small optical thickness value may translate into a long physical thickness for clouds such as thin Cirrus due to the long average distance between two successive scatterings for these clouds [18]. Note that, all the results presented in this paper assume a homogeneous body of clouds. In reality, as a waveform moves through clouds, the dynamics are far more rapidly varying. Hence, the predictions in this paper are on the conservative side.

VI. CONCLUSIONS

To answer the fundamental question of feasibility of optical communications in a scattering medium, one has to accurately model atmospheric optical channel and estimate parameters such as angular, spatial, and temporal dispersions. As a collimated laser beam propagates through aerosols and cloud particles, it spreads after traveling some optical thickness value and approaches a steady-state condition of being nearly spatially diffuse. The rate of convergence to this steady-state determines the feasibility of communications through various types of clouds and aerosols with different optical thickness values. Average distance between two successive scattering events is used to convert optical thickness of a specific scattering medium into its physical thickness and vice versa.

By directly applying Markov chain model to angular distribution evolution of laser beam in a scattering medium, and considering the fact that angular, spatial and temporal distributions of energy are inter-related, the mixing rate of Monte-Carlo Markov Chain (MCMC) is found for different types of scattering media. Mixing time is introduced as the

number of steps over which deviation from equilibrium state decreases by a factor e. This indicates the rate by which the energy distribution approaches being spatially isotropic. Examining parameters of Table-III, we realize that mixing time is rather short for clouds and haze. That is, when coherent light is traveling through clouds, its spatial coherence rapidly degrades. However, it may take a much larger cloud length value for the coherence bandwidth of the medium to vanish. In the latter case, optical pulses broaden extensively in time and restoring them by signal processing might be difficult.

ACKNOWLEDGMENTS

A DARPA Grant sponsored by the U.S. Air Force Research Laboratory/Wright-Patterson AFB Contract-FA8650-08-C-7850 and The Pennsylvania State University CICTR has supported this research. The authors would like to sincerely thank Dr. Graham J Martin of Teledyne Technologies Inc for many interesting discussions, Dr Larry Stotts, Deputy Director, Strategic Technology Office at DARPA and Mr. Brian Stadler of AFRL/RYJM for motivating the investigation. The paper is approved for Public Release, Distribution Unlimited.

REFERENCES

[1] B. Hamzeh and M. Kavehrad, "Laser Communication System Using Wavelet-Based Multi-Rate Signaling," *Proc. IEEE MILCOM,* Vol. 1, pp. 398-403, Monterey-California, November 2004.

[2] B. Hamzeh, and M. Kavehrad, "CDMA coded Free Space Optical Links for Wireless Optical Mesh Networks" *IEEE Trans. Commun.,* Vol. 52, No. 12, pp. 2165-2174, December 2004.

[3] B. Wu, B. Marchant, and M. Kavehrad, "Channel modeling of light signals propagating through a battlefield environment: analysis of channel spatial, angular, and temporal dispersion," *Applied Optics,* Vol. 46, No. 25, 6442-6448, Aug. 2007.

[4] Z. Hajjarian, M. Kavehrad, "Using MIMO Transmissions in Free Space Optical Communications in Presence of Clouds and Turbulence," *Proc. SPIE Photonics West,* San Jose, C.A. , January 2009.

[5] M. Wolf, and D. Kreb, "Short-Range Wireless Infrared Transmission: The Link Budget Compared to RF," *IEEE Wireless Commun.,* Vol.10, No .2, pp.8-14, April 2003.

[6] E. A. Bucher, R. M. Lerner,"Experiments on Light Pulse Communication and Propagation through Atmospheric Clouds" *Appl. Opt.* Vol. 12, No. 10, pp 2401-2414, October 1973.

[7] E. A. Bucher, "Computer simulation of light pulse propagation for communication through thick clouds," Appl. Opt, Vol. 12, No. 10, pp. 2391-2400. October 1973.

[8] N. S. Kopeika and J. Bordogna, "Background noise in optical communication systems," Proc. IEEE, Vol. 58, No. 10, pp. 1571-1577, October 1970.

[9] R. F. Lutomirski, A. P. Ciervo, and G. J. Hall, "Moments of multiple scattering," Appl. Opt., Vol. 34, No. 30, 7125-7136, October 1995.

[10] G. N. Plass,and G. W. Kattawar, "Monte Carlo calculations of light scattering from clouds," *Appl. Opt.,* Vol. 7, No. 3, pp. 415-419, March 1968.

[11] H. M. Gupta, "Space-time response of a cloud communication channel to an optical signal," *Optical and Quantum Electronics,* Vol. 12, No. 6, pp 499-509, November 1980.

[12] S. Arnon, D. Sadot, and N. S. Kopeika, "Simple mathematical models for temporal, spatial, angular characteristics of light propagating through the atmosphere for space optical communication: Monte Carlo simulations," *J. Mod. Opt.,* Vol. 41, pp. 1955-1972, Oct. 1994.

[13] S. Arnon, and N. S. Kopeika, "Free space optical communication: analysis of spatial widening of optical pulses for propagation through clouds," *Opt. Eng.,* Vol. 34, pp. 511-516, Feb. 1995.

[14] K. Riley, D. Ebert, M. Kraus, J. Tessendorf, and C. Hansen, "Efficient rendering of atmospheric phenomena," *Proc. Eurographics Symposium on Rendering 2004,* pp. 375-386, June 2004.

[15] F. G. Smith, *The Infrared & Electro-optical Systems Handbook: Atmospheric Propagating of Radiation,* Vol. 2, SPIE PRESS, 1993.

[16] D. Deirmendjian, "Scattering and Polarization Properties of Water Clouds and Hazes in the Visible and Infrared," *Appl. Opt.* Vol. 3, No. 2, pp 187-196, February 1964.

[17] A. Sawetprawichkul,P. Hsu, and K. Mitra, "Parallel Computing of Three-Dimensional Monte Carlo Simulation of Transient Radiative Transfer in Participating Media," *American Institute of Aeronautics and Astronautics,* 8th AIAA/ASME Joint Thermophysics and Heat Transfer Conference, St. Louis, Missouri, June 2002.

[18] B. Y. Hamzeh, *Multi-rate Wireless Optical Communications in Cloud Obscured Channels,* Ph.D. Thesis, Pennsylvania State University, December 2005.

[19] T. Binzoni, T. S. Leung, A. H. Gandjbakhche, D. Rfenacht,and D. T. Delpy, "The use of the Henyey-Greenstein phase function in Monte Carlo simulations in biomedical optics," *Physics in Medicine and Biology,* Vol. 51, No. 17, pp. N313-N322, Sepember 2006.

[20] T. Binzoni, T. S. Leung, A. H. Gandjbakhche, D. Rfenacht, and D. T. Delpy, "Comment on 'The use of the Henyey-Grenstein phase function in Monte Carlo simulations in biomedical optics," *Physics in Medicine and Biology,* Vol. 51, No. 22, pp. L39-L41(1), November 2006.

[21] L. Henyey, and J. Greenstein, "Diffuse radiation in the galaxy," *Astrophys. Journal,* Vol. 93, pp. 70-83, 1941.

[22] E. Behrends, *Introduction to Markov chains with special emphasis on rapid mixing,* Berlin, Friedrick Vieweg & Son, 2001.

[23] S. Boyd, P. Diaconis, and L. Xiao, "Fastest Mixing Markov Chain on a Graph," *SIAM Review,* Vol. 46, No. 4, pp. 667-689, December 2004.

[24] B. Wu, *Free-Space Optical Communications Through The Scattering Medium: Analysis of Signal Characteristics,* Ph.D. Thesis, Pennsylvania State University, December 2007.

Z. Hajjarian is a Ph.D. student in the Electrical Engineering Department, Center for Information and Communication Technology Research (CICTR), The Pennsylvania State University, University Park, PA.

Mohsen Kavehrad (F' 92) received his Ph.D. degree from Polytechnic University (Brooklyn Polytechnic), Brooklyn, New York, November 1977 in Electrical Engineering. Between 1978 and 1989, he worked on telecommunications problems for Fairchild Industries, GTE (Satellite and Labs.) and AT&T Bell Laboratories. In 1989, he joined the University of Ottawa EE Department, as a full professor. Since January 1997, he has been with the Pennsylvania State University EE Department as W.L. Weiss Chair Professor and founding Director of Center for Information and Communications Technology Research. He is a Fellow of the IEEE for his contributions to wireless communications and optical networking. He received 3 Bell Labs awards for his contributions to wireless communications, the 1990 TRIO feedback award for a patent on an optical interconnect, 2001 IEEE VTS Neal Shepherd best paper award, 3 IEEE Lasers and Electro-Optics Society best paper awards between 1991-95 and a Canada NSERC PhD-thesis award in 1995, with his graduate students for contributions to wireless systems and optical networks. He has over 300 published papers, several book chapters, books, and patents in these areas. His current research interests are in wireless communications and optical networks. He is a former Technical Editor for the IEEE Transactions on Communications, IEEE Communications Magazine and the IEEE Magazine of Light wave Telecommunications Systems. Presently, he is on the Editorial Board of the International Journal of Wireless Information Networks.

J. Fadlullah is a Ph.D. student in the Electrical Engineering Department, Center for Information and Communication Technology Research (CICTR), The Pennsylvania State University, University Park, PA.